Effective capillary interaction of spherical particles at fluid interfaces

M. Oettel, A. Domínguez, and S. Dietrich
Max-Planck-Institut für Metallforschung, Heisenbergstr. 3, D-70569 Stuttgart, Germany
and Institut für Theoretische und Angewandte Physik, Universität Stuttgart, Pfaffenwaldring 57, D-70569 Stuttgart, Germany
(Received 12 November 2004; published 12 May 2005)

We present a detailed analysis of the effective force between two smooth spherical colloids floating at a fluid interface due to deformations of the interface in an inhomogeneous pressure field. The results hold in general and are applicable independently of the source of the deformation provided the capillary deformations are small so that a superposition approximation for the deformations is valid. We conclude that an effective long-ranged attraction is possible if the net force on the system does not vanish. Otherwise, the interaction is short ranged and cannot be computed reliably based on the superposition approximation. As an application, we consider the case of like-charged, smooth nanoparticles and electrostatically induced capillary deformation. The resulting long-ranged capillary attraction can be easily tuned by a relatively small external electrostatic field, but it cannot explain recent experimental observations of attraction if these experimental systems were indeed isolated.

DOI: 10.1103/PhysRevE.71.051401 PACS number(s): 82.70.Dd

I. INTRODUCTION

In view of various applications such as the study of two-dimensional melting [1], investigations of mesoscale structure formation [2] or engineering of colloidal crystals on spherical surfaces [3], the self-assembly of sub-micrometer colloidal particles at water-air or water-oil interfaces has gained much interest in recent years. These particles are trapped at the interface if the colloid is only partially wetted by both the water and the oil. This configuration is stable against thermal fluctuations and appears to be the global equilibrium state, as it is observed experimentally that the colloids immersed in the bulk phases are attracted to the interface [1] (see also Sec. II). The mutual interaction between the trapped colloids at distances close to contact, i.e., within the range of molecular forces, is dominated by strong van der Waals attraction. In order to avoid coagulation due to this attraction, the colloids can be stabilized sterically with polymers or with charges such that the colloids repel each other. Variants of charge stabilization may include the coverage with ionizable molecules which dissociate in water, or the labeling of colloids with charged fluorescent markers. For charge-stabilized colloids at large distances, the resulting repulsive force at water interfaces stems from a dipole-dipole interaction as shown theoretically for point charges on surfaces [4] and verified experimentally for polystyrene (PS) spheres on water-oil interfaces [5].

Nonetheless, charged colloids at interfaces also show attractions far beyond the range of van der Waals forces. The corresponding experimental evidence can be roughly classified as follows. (i) According to Refs. [6–10], PS spheres (radii $R=0.25\cdots2.5\ \mu$m) on flat water-air interfaces using highly deionized water exhibit spontaneous formation of complicated metastable mesostructures. They are consistent with the presence of an attractive, secondary minimum in the intercolloidal potential at distances $d/R\approx3\cdots10$ with a depth of a few k_BT. The use of water slightly contaminated by ions seems to move the minimum further out and to reduce its depth [10,11]. (ii) In Ref. [12], poly(methylmethacrylate) (PMMA) spheres with radius $R=0.75\ \mu$m were trapped at the interface of water droplets immersed in oil. Here, the secondary minimum has been measured at a distance $d/R=7.6$ and is reported to be surprisingly steep. The tentative explanation of these findings given in Ref. [12] invokes an analog of long-ranged flotation or capilllary forces which decay $\propto1/d$. This interpretation was criticized in Ref. [13] (with which the authors of Ref. [12] agreed [14]) and in Ref. [15] which both concluded that possible capillary forces in this system are much shorter ranged, i.e., $\propto d^{-7}$, but the authors of these references disagree with respect to the sign of this shorter-ranged force. In yet another twist of the story, after completion of our work we encountered the very recent Ref. [16] in which the authors claim that long-ranged capillary forces $\propto1/d$ caused by the colloidal charges persist for submicrometer particles. This conclusion is based on measurements of the meniscus shape around single glass spheres with radii $200\cdots300\ \mu$m floating at water-oil and water-air interfaces.

Motivated by the experimental data summarized above and the still incomplete theoretical understanding, here we undertake a quite general analysis of capillary interactions between two spherical colloids trapped at fluid interfaces. Almost all previous studies have focused on the case of a constant pressure difference across the interface [17]. Our study generalizes the results for the capillary force by taking into account the effect of a spatially varying stress field acting on the interface; it also complements or corrects recent studies in the same direction [15,16]. We characterize the system by a general stress field, e.g., due to a discontinuous electrostatic field at the interface, and by a net force on the colloid, e.g., of gravitational or electrostatic origin. In Sec. II we present a free energy model for a single colloid trapped at an interface in the limit of small stresses and forces. The general solution for the interface deformation will be used in Sec. III in order to determine the effective potential between two colloids within the superposition approximation. In view of the differing theoretical results in the literature, the derivation of the interface deformation and the resulting effective

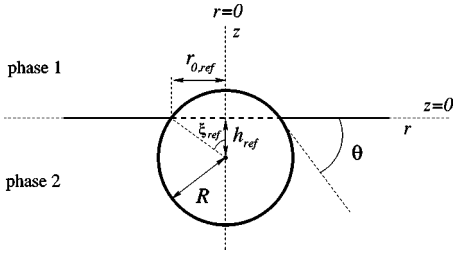

FIG. 1. Geometry of the reference state. The equilibrium contact angle θ fixes the height $h_{\mathrm{ref}}=-R\cos\theta$ of the colloid center, the contact radius $r_{0,\mathrm{ref}}=R\sin\theta$, and the auxiliary angular variable $\xi_{\mathrm{ref}}=\theta$.

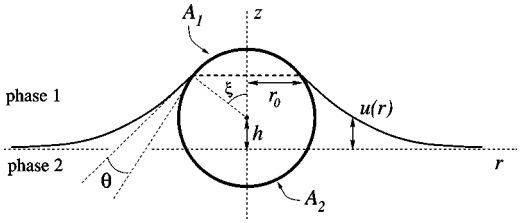

FIG. 2. Description of deviations from the reference state. $u(r)$ is the meniscus profile and h is the height of the colloid center. The angle ξ and the radius $r_0=R\sin\xi$ of the three-phase contact line are auxiliary variables, which depend on $u(r)$ and h through the geometrical relationship $h=u(r_0)-R\cos\xi$. In this mesoscopic description r_0 is defined as the position where the meniscus profile intersects the surface of the sphere. A_i is the surface area of the colloid exposed to phase i.

potential is presented in detail in order to reveal properly the subtleties involved. The presence of a long-ranged attractive capillary force $\propto 1/d$ is possible only if the system is not mechanically isolated, in which case the role of a restoring force fixing the interface, e.g., due to gravity or interface pinning, is essential. In Sec. IV we apply the results to the case of charged polymeric spheres on water interfaces. It turns out that the constraint of approximate mechanical isolation of the experimental systems renders the capillary interaction basically short ranged. In the context of our model, long-ranged attractive forces $\propto 1/d$ only arise in the presence of an external electric field. We shall discuss the relation to previous theoretical results, especially in view of the experimental results reported in Refs. [12,16]. Directions for further research will be pointed out. In Sec. V we summarize our results.

II. EQUILIBRIUM STATE OF A SINGLE COLLOID

In this section we consider as a first step the equilibrium state of a single colloid of radius R at the interface between two fluid phases denoted as 1 and 2. The contact angle formed by the interface and the colloid surface is given by Young's law

$$\cos\theta=\frac{\gamma_1-\gamma_2}{\gamma}, \tag{1}$$

where γ is the surface tension between phases 1 and 2, and γ_i is the surface tension between the colloid and phase i. As a reference state, with respect to which changes in free energy will be measured, we take a planar meniscus configuration with the colloid at such a height h_{ref} that Young's law is satisfied (Fig. 1). This corresponds to the equilibrium configuration of an uncharged colloid at the interface if its weight can be neglected—which for generic cases is a safe approximation for $R\lesssim 1$ μm [17] (see also Sec. IV). We model the colloid as a smooth sphere so that the system is invariant under rotations around the colloid axis perpendicular to the reference planar meniscus. The presence of charges induces a shift of the system (colloid and interface) with respect to the reference state. Here we neglect corresponding changes in the surface tensions γ and γ_i; this approximation is expected to be valid provided the concentration of charges is sufficiently small. This shift is characterized by the meniscus profile $u(r)$ relative to the planar configuration and by the height h of the colloid center. In the reference configuration, the charge distribution is assumed to be already in equilibrium. In the following we do not consider the degree of freedom "charge density field" explicitly but take it to be fixed to that of the reference configuration. This amounts to neglecting the feedback of the interface displacement on the charge distribution. It turns out to be useful to introduce the radius r_0 of the three-phase contact line and the angle ξ as auxiliary variables (see Fig. 2).

A. The free energy

In this subsection we formulate a free energy functional for the degrees of freedom $u(r)$ and h. As shown later, for the cases of interest here the deviations from the reference configuration are small enough to justify a perturbative treatment, and the free energy can be expanded up to quadratic order in $\Delta h:=h-h_{\mathrm{ref}}$ and $u(r)$. We denote with $\Pi(r)$ the vertical force per unit area acting on the meniscus surface in the reference configuration. In the case of a charged colloid, $\Pi(r)$ is given by the zz component of the difference of the Maxwell stress tensor right above and below the meniscus, plus the pressure difference acting across the meniscus (including an imbalance in osmotic pressure due to the different concentration of ions just above and below the meniscus) [15,18]. We introduce the following dimensionless parameter to measure the relative strength of this force:

$$\varepsilon_\Pi:=\frac{1}{2\pi\gamma r_{0,\mathrm{ref}}}\int_{S_{\mathrm{men,ref}}}dA\Pi=\frac{1}{\gamma r_{0,\mathrm{ref}}}\int_{r_{0,\mathrm{ref}}}^{\infty}drr\Pi(r), \tag{2}$$

where the integral extends over the flat meniscus $S_{\mathrm{men,ref}}$ (the plane $z=0$ with a circular hole of radius $r_{0,\mathrm{ref}}$). We assume $\Pi(r\to\infty)\sim r^{-n}$ with $n>2$, so that the integral converges. In the same spirit we introduce the total vertical force $\mathbf{F}=F\mathbf{e}_z$ acting on the charged colloid in the flat reference configuration, which includes gravity, the electrostatic force, and the total (i.e., hydrostatic and osmotic) pressure exerted by the fluids. This leads to the definition

$$\varepsilon_F := -\frac{F}{2\pi\gamma r_{0,\mathrm{ref}}}. \tag{3}$$

These two dimensionless parameters will appear naturally in the course of the calculations. If ε_Π and ε_F vanish, the reference configuration *is* the equilibrium state; it is the global minimum of the free energy functional given in Eqs. (4) and (13) below if $\Pi \equiv 0$, $F \equiv 0$. The aforementioned perturbative expansion of the free energy can be rephrased as an expansion in terms of the small parameters ε_Π and ε_F.

The free energy $\mathcal{F}$ of the colloid expressed relative to the reference configuration consists of five terms:

$$\mathcal{F} = \mathcal{F}_{\mathrm{cont}} + \mathcal{F}_{\mathrm{men}} + \mathcal{F}_{\mathrm{vol}} + \mathcal{F}_{\mathrm{inter}} + \mathcal{F}_{\mathrm{coll}}. \tag{4}$$

In the following we discuss each contribution.

Fluid contact of the colloid. With A_i denoting the surface area of the colloid which is in contact with phase i, the surface free energy of the colloid due to its exposure to the phases 1 and 2 is

$$\mathcal{F}_{\mathrm{cont}} = \gamma_1 A_1 + \gamma_2 A_2 - (\gamma_1 A_{1,\mathrm{ref}} + \gamma_2 A_{2,\mathrm{ref}}). \tag{5}$$

In Appendix A we express this contribution as a function of Δh and $u(r)$. The final result, valid up to corrections of at least third order in ε_Π or ε_F, reads

$$\mathcal{F}_{\mathrm{cont}} \simeq \pi\gamma[u(r_{0,\mathrm{ref}}) - \Delta h]^2 + \pi\gamma(r_0^2 - r_{0,\mathrm{ref}}^2). \tag{6}$$

Change of the meniscus area. The free energy contribution due to variations in the meniscus area relative to the reference state reads

$$\mathcal{F}_{\mathrm{men}} = \gamma\int_{S_{\mathrm{men}}} dA\sqrt{1+|\nabla u|^2} - \gamma\int_{S_{\mathrm{men,ref}}} dA, \tag{7}$$

where S_{men} is the surface of the fluid interface projected onto the plane $z=0$ (in which the reference interface is located), and ∇ is the gradient operator on the flat reference interface. For small slopes ($|\nabla u| \ll 1$) one obtains

$$\begin{aligned}\mathcal{F}_{\mathrm{men}} &\simeq \gamma\int_{S_{\mathrm{men}}\setminus S_{\mathrm{men,ref}}} dA + \tfrac{1}{2}\gamma\int_{S_{\mathrm{men}}} dA|\nabla u|^2 \\ &\simeq \pi\gamma(r_{0,\mathrm{ref}}^2 - r_0^2) + \tfrac{1}{2}\gamma\int_{S_{\mathrm{men,ref}}} dA|\nabla u|^2.\end{aligned} \tag{8}$$

Since the u-dependent term is of second order in u, we have approximated the integration domain S_{men} by $S_{\mathrm{men,ref}}$; the corrections are at least of third order in the small parameters ε_Π or ε_F. The first term in this expression represents the change in the area of the meniscus which is cut out by the colloid, and in Eq. (4) it cancels the second term of Eq. (6).

Volume forces on the fluids. We consider the case that the only volume force acting on the fluid phases is gravity. The electrostatic forces are active only at the surfaces, where a net charge can accumulate. First, there is a contribution due to the vertical displacement Δh of the colloid; this contribution is contained in $\mathcal{F}_{\mathrm{coll}}$ [see Eq. (12) below], since the total force F includes the buoyancy force. Second, there is the change in gravitational potential energy relative to the reference state due to the meniscus deformation $u(r)$. We assume that the mass density of phase 2 is larger than the one of phase 1, i.e., $\varrho_2 > \varrho_1$, and define the capillary length

$$\lambda := \sqrt{\frac{\gamma}{(\rho_2 - \rho_1)g}} \tag{9}$$

in terms of the acceleration g of gravity. This leads to (see Fig. 2):

$$\mathcal{F}_{\mathrm{vol}} = \frac{1}{2}\gamma\int_{S_{\mathrm{men,ref}}} dA\frac{u^2(r)}{\lambda^2} = \pi\gamma\int_{r_{0,\mathrm{ref}}}^{\infty} drr\frac{u^2(r)}{\lambda^2}, \tag{10}$$

plus corrections of third order in ε_Π, ε_F stemming from the fluid contained in the small volume $\sim r_{0,\mathrm{ref}}|u(r_{0,\mathrm{ref}})||r_0 - r_{0,\mathrm{ref}}|$.

As it will be shown in Sec. II C, the precise form of $\mathcal{F}_{\mathrm{vol}}$ is irrelevant in the limit $\lambda \to \infty$ ($\lambda \approx 1$ mm, which is much larger than any other relevant length scale in the systems we intend to study). Indeed, one can consider the functional form (10) just as the simplest mathematical way to achieve that the reference meniscus configuration $u(r) \equiv 0$ is well defined and stable when $\varepsilon_\Pi = \varepsilon_F = 0$.

Force on the fluid interface. The aforementioned surface force density $\Pi(r)$ acts on the fluid interface between phases 1 and 2. The free energy change due to the ensuing displacements of the meniscus is

$$\begin{aligned}\mathcal{F}_{\mathrm{inter}} &\simeq -\int_{S_{\mathrm{men}}} dA\Pi u \simeq -\int_{S_{\mathrm{men,ref}}} dA\Pi u \\ &= -2\pi\int_{r_{0,\mathrm{ref}}}^{\infty} drr\Pi(r)u(r).\end{aligned} \tag{11}$$

Here $\Pi(r)$ is the surface force in the *reference* configuration ($\Pi > 0$ corresponds to a force pointing upward). Changes in the force induced by meniscus deformations and colloidal displacements contribute terms of higher orders in ε_Π or ε_F in Eq. (11). The replacement of S_{men} by $S_{\mathrm{men,ref}}$ in Eq. (11) introduces terms of higher order, too.

Contribution from the colloid. The free energy change due to a vertical displacement of the colloid is

$$\mathcal{F}_{\mathrm{coll}} \simeq -F\Delta h, \tag{12}$$

where F is the vertical force on the colloid in the *reference* configuration. Like for $\mathcal{F}_{\mathrm{inter}}$, changes of F due to deviations from the reference configuration contribute to higher order terms.

In conclusion, by adding Eqs. (6), (8), and (10)–(12) we obtain the following approximate expression for the total free energy, which is correct up to second order in ε_Π or ε_F, and which is a function of Δh and a functional of $u(r)$:

$$\begin{aligned}\mathcal{F} \simeq{}& 2\pi\gamma\int_{r_{0,\mathrm{ref}}}^{\infty} drr\left[\frac{1}{2}\left(\frac{du}{dr}\right)^2 + \frac{u^2}{2\lambda^2} - \frac{1}{\gamma}\Pi u\right] + \pi\gamma[u_0 - \Delta h]^2 \\ &- F\Delta h,\end{aligned} \tag{13}$$

where $u_0 \equiv u(r_{0,\mathrm{ref}})$.

B. Minimization of the free energy

The equilibrium configuration of the system minimizes the free energy expression (13). The minimization proceeds in two stages. First we seek the minimum with respect to Δh at fixed $u(r)$:

$$\frac{\partial \mathcal{F}}{\partial(\Delta h)} = 0 \Rightarrow \Delta h = u_0 - \varepsilon_F r_{0,\mathrm{ref}}, \tag{14}$$

where we have used the definition (3). Using repeatedly the definitions of h and r_0 in terms of the auxiliary angle ξ (Fig. 2) we can compute the change of the contact radius,

$$\begin{aligned}\Delta r_0 &\equiv r_0 - r_{0,\mathrm{ref}} = R(\sin\xi - \sin\theta) \\ &\simeq (\theta - \xi) h_{\mathrm{ref}} \simeq \frac{\Delta h - u_0}{r_{0,\mathrm{ref}}} h_{\mathrm{ref}} = -\varepsilon_F h_{\mathrm{ref}},\end{aligned} \tag{15}$$

plus corrections of second order in ε_Π, ε_F. In the second step, we minimize Eq. (13) with respect to $u(r)$ at fixed Δh. This is a problem of variations with a free boundary condition at $r = r_{0,\mathrm{ref}}$ [19]. Variation with respect to $u(r \neq r_{0,\mathrm{ref}})$ yields a second-order ordinary differential equation

$$\frac{d^2u}{dr^2} + \frac{1}{r}\frac{du}{dr} - \frac{1}{\lambda^2}u = -\frac{1}{\gamma}\Pi(r), \tag{16}$$

while variation with respect to u_0 provides a boundary condition,

$$u_0' := \left.\frac{du}{dr}\right|_{r=r_{0,\mathrm{ref}}} = \frac{u_0 - \Delta h}{r_{0,\mathrm{ref}}} = \varepsilon_F, \tag{17}$$

where the last equality follows from Eq. (14). The second boundary condition one has to impose on Eq. (16) follows from the requirement that the meniscus is asymptotically flat far from the colloid (assuming that $\Pi(r \to \infty) = 0$):

$$\lim_{r\to\infty} u(r) = 0. \tag{18}$$

Equation (16) describes mechanical equilibrium of the interface such that the Laplace pressure balances the forces acting on the interface. The boundary condition (17) expresses mechanical equilibrium of the colloidal particle: At the contact line (i.e., the circle with radius r_0 at $z = u_0$) the interface exerts a force onto the colloid which has a nonvanishing contribution only in z direction with the magnitude $2\pi\gamma r_0 \sin[\arctan(u_0')] \approx 2\pi\gamma r_{0,\mathrm{ref}} u_0'$. This contact line force is balanced by the total force F.

The solution of Eqs. (16)–(18) can be written in terms of the modified Bessel functions of zeroth order

$$\begin{aligned}u(r) = &\frac{1}{\gamma} I_0\left(\frac{r}{\lambda}\right) \int_r^\infty ds s \Pi(s) K_0\left(\frac{s}{\lambda}\right) \\ &+ \frac{1}{\gamma} K_0\left(\frac{r}{\lambda}\right)\left[A + \int_{r_{0,\mathrm{ref}}}^r ds s \Pi(s) I_0\left(\frac{s}{\lambda}\right)\right],\end{aligned} \tag{19}$$

where the integration constant A is determined by the boundary condition (17).

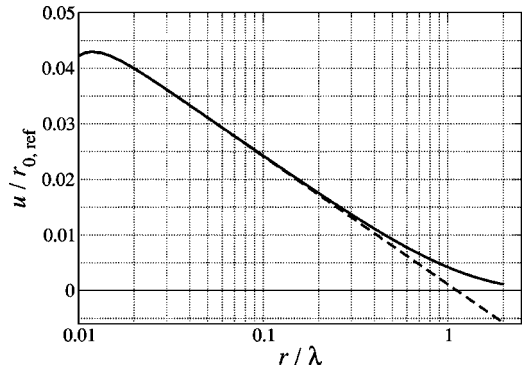

FIG. 3. The meniscus solution for the parameter choice $\lambda/r_{0,\mathrm{ref}} = 10^2$, $\varepsilon_F = 10^{-2}$, and a dipolelike stress field $r_{0,\mathrm{ref}}\Pi(r)/\gamma = 0.08(r_{0,\mathrm{ref}}/r)^6$ ($\varepsilon_\Pi = 2 \cdot 10^{-2}$). The solid line represents the solution $u(r)$ given by Eq. (19). The dashed line is the intermediate asymptotic solution given by Eq. (20). Note that the capillary length λ is typically of $O(1\ \mathrm{mm})$. In the present context we focus on the length scale $r_{0,\mathrm{ref}}, r \ll \lambda$, for which Eq. (20) holds.

C. Asymptotic behavior in the limit $\lambda \to \infty$

For typical values of the parameters, λ is of the order of millimeters and therefore much larger than any other length scale occurring for experiments with submicrometer colloids. In order to study the intermediate asymptotics ($r_{0,\mathrm{ref}}, r \ll \lambda$) of $u(r)$ as given by Eq. (19), we insert the asymptotic expansions of the Bessel functions [20] as $\lambda \to \infty$ and retain those terms which do not vanish in this limit. Assuming that $\Pi(r \to \infty)$ decays sufficiently fast, Eq. (19) reduces to

$$u(r) \simeq r_{0,\mathrm{ref}}(\varepsilon_\Pi - \varepsilon_F) \ln\frac{C\lambda}{r} - \frac{1}{\gamma}\int_r^{+\infty} ds s \Pi(s) \ln\frac{s}{r}, \tag{20}$$

where $C = 2e^{-\gamma_E} \simeq 1.12$ and γ_E is Euler's constant. In Eq. (20), we have expressed the integration constant A appearing in Eq. (19) in terms of ε_F by using the boundary condition (17). The first term in Eq. (20) is a solution of the homogeneous part of Eq. (16) (with $\lambda^{-1} = 0$ in the equation), demonstrating that the limit $\lambda \to \infty$ is singular as long as $\varepsilon_\Pi \neq \varepsilon_F$. The second term corresponds to a particular solution of the inhomogeneous differential equation. If the surface force $\Pi(r)$ decays algebraically, $\Pi(r \to \infty) \propto r^{-n}$, this term decays like r^{2-n} (since we have assumed $n > 2$), so that the logarithmic contribution is dominant. If $n \leqslant 2$, the asymptotic behavior is no longer given by Eq. (20) but a different dependence on λ arises.

At distances r of the order of λ, the expression (20) is not valid and a crossover to the exact solution (19) takes place in order to satisfy the boundary condition at infinity [Eq. (18)]. Figure 3 sketches the behavior of the meniscus profile $u(r)$. As can be checked directly in the differential Eq. (16), one has $u(r) \sim (\lambda^2/\gamma)\Pi(r) \propto r^{-n}$ asymptotically as $r \to +\infty$, which expresses the balance between the surface force $\Pi(r)$ on the meniscus and the gravitational force. There is, however, another intermediate regime $r \gg \lambda$ but not too large, in which $u(r)$ decays $\propto \exp(-r/\lambda)$ and which corresponds to the solution of Eq. (16) with Π set to zero, i.e., when gravity is

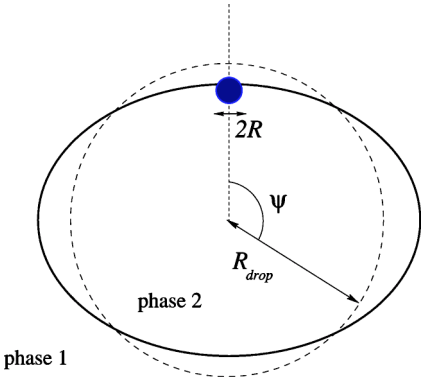

FIG. 4. Colloid at the surface of a droplet of phase 2 immersed into phase 1. The radius R_{drop} of the droplet, which is spherical without the colloid, is usually much larger than the colloid radius R. (The deformation of the droplet has been exaggerated.)

balanced by the Laplace pressure induced by the meniscus curvature.

These conclusions, as well as the functional dependence of $u(r)$ on $\Pi(r)$, are robust and independent of the details of the boundary condition at $r\to\infty$. In order to support this statement, we consider two cases which implement the distant boundary condition differently.

Pinned interface. In the absence of gravity the interface is assumed to be pinned at a finite distance L from the colloid. This corresponds to setting $\lambda^{-1}=0$ in Eq. (16) and replacing Eq. (18) by the boundary condition $u(L)=0$. In this case the solution of Eq. (16) is given by

$$u(r)=r_{0,\mathrm{ref}}(\tilde{\varepsilon}_{\Pi}-\varepsilon_F)\ln\frac{L}{r}-\frac{1}{\gamma}\int_r^L dss\Pi(s)\ln\frac{s}{r}, \qquad (21)$$

where

$$\tilde{\varepsilon}_{\Pi}:=\frac{1}{\gamma r_{0,\mathrm{ref}}}\int_{r_{0,\mathrm{ref}}}^{L}drr\Pi(r), \qquad (22)$$

in analogy to Eq. (2). In the intermediate asymptotic regime $(r_{0,\mathrm{ref}},r\ll L)$, the meniscus profile is then given by

$$u(r)\simeq r_{0,\mathrm{ref}}(\varepsilon_{\Pi}-\varepsilon_F)\ln\frac{L}{r}-\frac{1}{\gamma}\int_r^{+\infty}dss\Pi(s)\ln\frac{s}{r}, \qquad (23)$$

assuming that $\Pi(r)$ decays sufficiently fast so that the integrals in Eqs. (21) and (22) converge as $L\to\infty$. Equation (23) resembles Eq. (20) with $C\lambda$ replaced by L.

Pinned curved reference interface. In some experiments the interface between phases 1 and 2 is in fact closed, so that the colloidal particle lies at the surface of a large nonvolatile spherical droplet of phase 2 which is immersed in phase 1 [12] (Fig. 4) and fixed by certain means (e.g., by a glass plate). The free energy functional (13) has to be modified to account for the curvature of the reference interface as well as for the constraint that the droplet volume remains unchanged under deformation. To determine the interface deformation, we minimize the functional and employ the boundary condition that the droplet is fixed at some point far from the colloid. The mathematical details and the corresponding solution for $u(r)$ are presented in Appendix B. Here we quote only the intermediate asymptotic behavior $(r_{0,\mathrm{ref}},r\ll R_{\mathrm{drop}}$, where R_{drop} is the radius of the undeformed droplet):

$$u(r)\simeq r_{0,\mathrm{ref}}(\varepsilon_{\Pi}-\varepsilon_F)\ln\frac{\tilde{C}R_{\mathrm{drop}}}{r}-\frac{1}{\gamma}\int_r^{+\infty}dss\Pi(s)\ln\frac{s}{r}, \qquad (24)$$

with $\tilde{C}$ a numerical constant given by Eq. (B23). Again Eq. (24) closely resembles Eqs. (20) and (23).

The physical reason for the occurrence of the singularity in the limit $\lambda, L, R_{\mathrm{drop}}\to+\infty$ is that a "restoring force" far from the particle is required to yield a well-defined unperturbed interface which allows one to determine the deformation $u(r)$ unambiguously. For example, if one takes the limit $\lambda\to+\infty$ in the Young-Laplace Eq. (16), it is inconsistent to impose the boundary condition $u(r\to+\infty)=0$ in the corresponding solution. The special case $\varepsilon_{\Pi}=\varepsilon_F$, however, is not singular; this will be discussed in Sec. IV. Furthermore, the comparison of Eqs. (20), (23), and (24) demonstrates that the functional form of the intermediate asymptotic behavior is independent of how the restoring force is implemented. This corresponds to the so-called intermediate asymptotic behavior of the second kind [21], characterized by the following features.

(1) There is a length scale (λ, L, or R_{drop}) which is much larger than the other length scales of the system under consideration and which seems—at first sight—to be irrelevant.

(2) Nevertheless, this length scale determines the dominant logarithmic (or more generally, the power law) dependence.

(3) The detailed physical origin of this length scale (in the examples we have considered, gravity, pinning of a reference flat or curved interface) does not matter.

Well known examples of this kind of asymptotic behavior are critical phenomena in phase transitions [22]. In that case, it is the microscopic length scale given by the amplitude of the correlation length which cannot be set to zero although it is much smaller than the correlation length itself. This microscopic length scale is required to formulate the power-law behavior of certain properties of the system, but its detailed physical origin is unimportant for the universal decay exponents of the power laws.

III. EFFECTIVE INTERACTION POTENTIAL OF TWO FLOATING COLLOIDS

In this section we consider the equilibrium state of two identical colloids floating at the interface at a fixed lateral distance d and compute the effective interaction potential $V_{\mathrm{men}}(d)$ generated by the meniscus. The free energy can be derived along the same lines leading to Eq. (13), but with due account for the fact that in the presence of two colloids the meniscus slope no longer exhibits rotational symmetry. Nonetheless V_{men} depends only on the distance d between the centers of the two spheres. The reference configuration is that of two colloids floating on a planar interface with the corresponding reference free energy being independent of d.

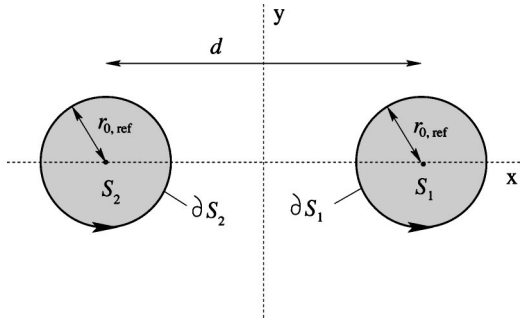

FIG. 5. Top view (projection onto the plane $z=0$) of the reference configuration with two colloids. d is the distance between the colloid centers. S_1 and S_2 are disks of radius $r_{0,\mathrm{ref}}$, the corresponding circumferences (counterclockwise) are ∂S_1 and ∂S_2. The projection of the interface is $S_{\mathrm{men,ref}}=\mathbb{R}^2\backslash(S_1\cup S_2)$.

In this case one has for the free energy relative to that of the reference configuration a contribution $\mathcal{F}_{\mathrm{men}}+\mathcal{F}_{\mathrm{vol}}+\mathcal{F}_{\mathrm{inter}}$ from the meniscus and a contribution of the form $\mathcal{F}_{\mathrm{cont}}+\mathcal{F}_{\mathrm{coll}}$ from each colloid. (The total free energy includes also the direct interaction between the colloids; this contribution will be considered in Sec. IV B). From Eqs. (A7), (8), and (10)–(12) one obtains

$$\hat{\mathcal{F}} \simeq \gamma \int_{\mathbb{R}^2\backslash(S_1\cup S_2)} dA \left[\frac{1}{2} |\nabla \hat{u}|^2 + \frac{\hat{u}^2}{2\lambda^2} - \frac{1}{\gamma}\hat{\Pi}\hat{u} \right] + \sum_{\alpha=1,2} \left\{ \frac{\gamma}{2r_{0,\mathrm{ref}}} \oint_{\partial S_\alpha} d\ell [\Delta\hat{h}_\alpha - \hat{u}]^2 - \hat{F}_\alpha \Delta\hat{h}_\alpha \right\}. \quad (25)$$

Here, $\hat{u}$ is the meniscus profile in the presence of two colloids, $\Delta\hat{h}_\alpha$ are the corresponding heights, $\hat{\Pi}$ is the vertical force per unit area on the meniscus in the reference configuration, and $\hat{F}_\alpha$ is the force on each colloid. By symmetry, one has $\Delta\hat{h}_1=\Delta\hat{h}_2$ and $\hat{F}_1=\hat{F}_2$. S_α are the circular disks delimited by the contact lines of the colloids in the reference configuration, ∂S_α are the contact lines, with the convention that we trace them counterclockwise, and $S_{\mathrm{men,ref}}=\mathbb{R}^2\backslash(S_1\cup S_2)$ (see Fig. 5).

A. Minimization of the free energy within the superposition approximation

The equilibrium configuration is the minimum of the free energy given by Eq. (25). The minimization procedure follows closely Sec. II B. First, minimizing with respect to $\Delta\hat{h}_\alpha$ at fixed meniscus height $\hat{u}$ leads to the height of the colloids,

$$\frac{\partial \mathcal{F}}{\partial(\Delta h_\alpha)} = 0 \Rightarrow \Delta\hat{h}_\alpha = \overline{\hat{u}}_\alpha - \varepsilon_{\hat{F}} r_{0,\mathrm{ref}}, \quad (26)$$

where

$$\overline{\hat{u}}_\alpha := \frac{1}{2\pi r_{0,\mathrm{ref}}} \oint_{\partial S_\alpha} d\ell\, \hat{u} \quad (27)$$

is the mean height of the contact line. In the next step, we minimize with respect to $\hat{u}$ at fixed $\Delta\hat{h}_\alpha$. Variation in the interior of the domain $\mathbb{R}^2\backslash(S_1\cup S_2)$ provides a second-order partial differential equation

$$\nabla^2\hat{u} - \frac{1}{\lambda^2}\hat{u} = -\frac{1}{\gamma}\hat{\Pi}, \quad (28)$$

while variation at the boundary $\partial S_1\cup\partial S_2$ provides the following *transversality conditions* [19]:

$$\frac{\partial\hat{u}(\mathbf{r})}{\partial n_\alpha} = \frac{\hat{u}(\mathbf{r})-\Delta\hat{h}_\alpha}{r_{0,\mathrm{ref}}} = \varepsilon_{\hat{F}} + \frac{\hat{u}(\mathbf{r})-\overline{\hat{u}}_\alpha}{r_{0,\mathrm{ref}}}, \quad \mathbf{r}=(x,y)\in\partial S_\alpha, \quad (29)$$

where the last equality follows from Eq. (26). In this expression, $\partial/\partial n_\alpha$ is the derivative in the outward normal direction of ∂S_α. [In this way, the triad $(\mathbf{e}_n,\mathbf{e}_t,\mathbf{e}_z)$ is right-handed, where $\mathbf{e}_n$ is the unit vector in the outward normal direction, $\mathbf{e}_t$ is the unit vector in the counterclockwise tangent direction, and $\mathbf{e}_z$ is the unit vector in the positive z direction.] When applying the transversality condition, in the context of Gauss' theorem one must keep in mind that the boundary of the region $\mathbb{R}^2\backslash(S_1\cup S_2)$ consists of the contours ∂S_α traced in *clockwise direction* with the normals directed towards the interior of S_α. [The boundary at $r\to\infty$ does not contribute due to Eq. (30).] In the special case of a single colloid, rotational invariance reduces Eq. (29) to Eq. (17). Finally, one has the additional boundary condition

$$\lim_{r\to\infty}\hat{u}(\mathbf{r}) = 0. \quad (30)$$

The solution of Eq. (28) with the boundary conditions given by Eqs. (29) and (30) is a difficult task. [We are only aware of the—already very involved—solution of the homogeneous Eq. (28), i.e., $\hat{\Pi}=0$, with the simplified boundary condition $\partial\hat{u}/\partial n_\alpha=\varepsilon_{\hat{F}}$ [23].] For the present purpose, one can use the so-called *superposition approximation* [25,24,26], which yields the correct solution in the asymptotic limit of large separation $d\gg R$ between the colloids. Let u_α denote the equilibrium meniscus profile as if colloid α was alone, with Π_α and F_α denoting the corresponding forces. The superposition approximation then reads:

$$\hat{u} \simeq u_1 + u_2,$$

$$\hat{\Pi} \simeq \Pi_1 + \Pi_2, \quad (31)$$

$$\hat{F} \simeq F_1 = F_2.$$

Notice that the fields $u_\alpha(\mathbf{r})$ and $\Pi_\alpha(\mathbf{r})$ are defined in the domain $\mathbb{R}^2\backslash S_\alpha$, while the fields $\hat{u}(\mathbf{r})$ and $\hat{\Pi}(\mathbf{r})$ are defined in the smaller domain $\mathbb{R}^2\backslash(S_1\cup S_2)$. Equations (28) and (30) are

fulfilled by this approximate solution, but the boundary condition (29) is violated: using Eqs. (31) and the boundary condition in Eq. (17) for the single-colloid solution, one obtains

$$\left[\frac{\partial\hat{u}(\mathbf{r})}{\partial n_1}-\varepsilon_{\hat{F}}-\frac{\hat{u}(\mathbf{r})-\overline{\hat{u}_1}}{r_{0,\mathrm{ref}}}\right]_{\mathbf{r}\in\partial S_1} \simeq \left[\frac{\partial u_2(\mathbf{r})}{\partial n_1}-\frac{1}{r_{0,\mathrm{ref}}}\left\{u_2(\mathbf{r})-\frac{1}{2\pi r_{0,\mathrm{ref}}}\oint_{\partial S_1}d\ell u_2\right\}\right]_{\mathbf{r}\in\partial S_1}, \tag{32}$$

and a similar expression for the other colloid with the indices 1 and 2 interchanged. In general, this expression does not vanish as required by Eq. (29). If d is large, Eq. (32) can be evaluated by expanding u_2 into a Taylor series around the center of colloid 1, yielding to lowest order ($\mathbf{e}_1$ is the outward directed normal unit vector of ∂S_1)

$$\left[\frac{\partial\hat{u}(\mathbf{r})}{\partial n_1}-\varepsilon_{\hat{F}}-\frac{\hat{u}(\mathbf{r})-\overline{\hat{u}_1}}{r_{0,\mathrm{ref}}}\right]_{\mathbf{r}\in\partial S_1} \simeq \frac{1}{4}r_{0,\mathrm{ref}}[\mathbf{e}_1\mathbf{e}_1\colon\boldsymbol{\nabla}\,\boldsymbol{\nabla}\,u_2(d)+\boldsymbol{\nabla}^2u_2(d)] \tag{33}$$

in dyadic notation. Inserting the single-colloid solution given in Eq. (20), one finds that this expression decays like d^{-2} if $\varepsilon_F\neq\varepsilon_\Pi$, and like $\Pi(d)\sim d^{-n}$ if $\varepsilon_F=\varepsilon_\Pi$.

The superposition solution can be used to determine the vertical displacement according to Eq. (26):

$$\Delta\hat{h}_\alpha\simeq\Delta h+\overline{u}, \tag{34}$$

where Δh is the relative vertical displacement of an isolated colloid [Eq. (14)] and

$$\overline{u}:=\frac{1}{2\pi r_{0,\mathrm{ref}}}\oint_{\partial S_1}d\ell u_2 \tag{35}$$

is the average of the single-colloid meniscus height at the contact line of the other colloid.

B. Effective interaction potential

The meniscus-induced effective potential between the two colloids (without their direct interaction) is defined as

$$V_{\mathrm{men}}(d):=\hat{\mathcal{F}}-\mathcal{F}_1-\mathcal{F}_2, \tag{36}$$

where $\hat{\mathcal{F}}$ is the free energy of the two-colloid equilibrium configuration [Eq. (25)] while $\mathcal{F}_1=\mathcal{F}_2$ is the single-colloid equilibrium free energy [Eq. (13)]. As noted before the energy of the reference configuration is independent of the separation d and drops out from Eq. (36). We insert Eqs. (31), (34), and (35) into Eq. (36) and exploit the invariance of the free energy under exchange of the colloids, i.e., the symmetry under exchanging indices $1\leftrightarrow2$. After carrying out some analytic manipulations one finds the following expression for the effective potential:

$$\begin{aligned}V_{\mathrm{men}}(d)\simeq&\int_{\mathbb{R}^2\setminus(S_1\cup S_2)}dA\left[\gamma(\boldsymbol{\nabla}u_1)\cdot(\boldsymbol{\nabla}u_2)+\frac{\gamma}{\lambda^2}u_1u_2-2\Pi_1u_2\right]\\&-\int_{S_1}dA\left[\gamma|\boldsymbol{\nabla}u_2|^2+\frac{\gamma}{\lambda^2}u_2^2-2\Pi_2u_2\right]\\&+\frac{\gamma}{r_{0,\mathrm{ref}}}\oint_{\partial S_1}d\ell[\overline{u}-u_2]^2-2F\overline{u}.\end{aligned} \tag{37}$$

The first integral accounts for the change in surface energy, gravitational potential energy, and surface-stress potential energy of the meniscus due to the overlap of the meniscus deformations caused by the two colloids. The second integral is the corresponding change due to the fact that the interface is reduced by an amount S_1 compared to the single-colloid case because of the presence of the second colloid. The third integral is the change in surface free energy of one colloid due to the extra meniscus deformation induced by the second colloid. The last term is the change in energy due to the vertical displacement of one colloid by this extra meniscus deformation.

For the mathematical manipulations to follow, it is suitable to rewrite Eq. (37) by applying Gauss' theorem to the integrals involving $\boldsymbol{\nabla}u$ and by using the fact that the functions u_α fulfill Eq. (16) individually, e.g.,

$$\begin{aligned}&\gamma\int_{\mathbb{R}^2\setminus(S_1\cup S_2)}dA(\boldsymbol{\nabla}u_1)\cdot(\boldsymbol{\nabla}u_2)\\&=\gamma\int_{\mathbb{R}^2\setminus(S_1\cup S_2)}dA[\boldsymbol{\nabla}\cdot(u_2\,\boldsymbol{\nabla}u_1)-u_2\boldsymbol{\nabla}^2u_1]\\&=-\gamma\oint_{\partial S_1}d\ell\frac{\partial(u_1u_2)}{\partial n_1}+\int_{\mathbb{R}^2\setminus(S_1\cup S_2)}dA\left[\Pi_1u_2-\frac{\gamma}{\lambda^2}u_1u_2\right].\end{aligned} \tag{38}$$

Thus one obtains from Eq. (37):

$$\begin{aligned}V_{\mathrm{men}}(d)\simeq&-\int_{\mathbb{R}^2\setminus(S_1\cup S_2)}dA\Pi_1u_2+\int_{S_1}dA\Pi_2u_2\\&-\gamma\oint_{\partial S_1}d\ell\frac{\partial(u_1u_2)}{\partial n_1}-\frac{1}{2}\gamma\oint_{\partial S_1}d\ell\frac{\partial u_2^2}{\partial n_1}\\&+\frac{\gamma}{r_{0,\mathrm{ref}}}\oint_{\partial S_1}d\ell[\overline{u}-u_2]^2-2F\overline{u}.\end{aligned} \tag{39}$$

In this form all the integrals, except the first one, are performed over bounded domains. This allows one to carry out a Taylor expansion which yields a uniformly valid asymptotic expansions of the terms as $d\to\infty$. In the following calculations, the integrals are evaluated in polar coordinates with the origin at the center of S_α and $\mathbf{r}_\alpha$ is the position vector with respect to this origin. In particular, $\mathbf{r}_2=d\mathbf{e}_x$ is the center of colloid 1 with respect to the center of colloid 2, and $\mathbf{r}_1=-d\mathbf{e}_x$ is the center of colloid 2 with respect to the center of colloid 1 (Fig. 5) so that, e.g., $u_\alpha=u(|\mathbf{r}_\alpha|)$.

(1) In order to compute the leading asymptotic behavior of the first term in Eq. (39) as $d\to\infty$ we distinguish two cases.

(a) $\varepsilon_\Pi \neq \varepsilon_F$: In this case, $u\sim\log r$ [Eq. (20)] while $\Pi \sim r^{-n}$ $(n>2)$ as $r\to\infty$. Asymptotically the main contribution stems from the region near S_1 and

$$\int_{\mathbb{R}^2\setminus(S_1\cup S_2)} dA\Pi_1 u_2 \simeq u(d)\int_{\mathbb{R}^2\setminus S_1} dA\Pi_1 = 2\pi\gamma r_{0,\mathrm{ref}}\varepsilon_\Pi u(d), \tag{40}$$

employing the definition (2). It will turn out that there is no need to compute also the next-to-leading term in order to obtain $V_{\mathrm{men}}(d\to\infty)$, as the leading term will be part of the leading contribution to V_{men} and it will not be cancelled by other contributions.

(b) $\varepsilon_\Pi=\varepsilon_F$: In this case $u\sim r^{2-n}$ if $\Pi(r\to\infty)\sim r^{-n}$. The regions contributing mainly to the integral are the neighborhoods of S_1 and S_2. We employ the Taylor expansion of the integrand (which is valid up to a maximum order depending on how fast Π decays) to evaluate the leading and the next-to-leading contributions if $n>4$ (using dyadic notation):

$$\begin{aligned}\int_{\mathbb{R}^2\setminus(S_1\cup S_2)} dA\Pi_1 u_2 \simeq& \int_{\mathbb{R}^2\setminus S_1} dA\Pi_1[u_2+\mathbf{r}_1\cdot(\boldsymbol{\nabla}u)_2\\ &+\tfrac{1}{2}\mathbf{r}_1\mathbf{r}_1:(\boldsymbol{\nabla}\boldsymbol{\nabla}u)_2+\cdots]_{\mathbf{r}_2=d\mathbf{e}_x}\\ &+\int_{\mathbb{R}^2\setminus S_2} dAu_2[\Pi_1+\cdots]_{\mathbf{r}_1=-d\mathbf{e}_x}\\ \simeq& 2\pi\gamma r_{0,\mathrm{ref}}\varepsilon_\Pi u(d)\\ &+\tfrac{1}{2}\pi\boldsymbol{\nabla}^2u(d)\int_{r_{0,\mathrm{ref}}}^\infty drr^3\Pi(r)\\ &+\Pi(d)\int_{\mathbb{R}^2\setminus S_2} dAu_2+\cdots.\end{aligned} \tag{41}$$

We can simplify the result further by evaluating the last integral by repeated partial integration with the explicit solution for u given in Eq. (20):

$$\begin{aligned}\int_{\mathbb{R}^2\setminus S_2} dAu(r_2) =& \frac{1}{2}\pi r_{0,\mathrm{ref}}^3\left[\varepsilon_\Pi-\frac{2u_0}{r_{0,\mathrm{ref}}}\right.\\ &\left.-\frac{1}{\gamma r_{0,\mathrm{ref}}^3}\int_{r_{0,\mathrm{ref}}}^\infty drr^3\Pi(r)\right].\end{aligned} \tag{42}$$

One finally obtains

$$\begin{aligned}\int_{\mathbb{R}^2\setminus(S_1\cup S_2)} dA\Pi_1 u_2 \simeq& 2\pi\gamma r_{0,\mathrm{ref}}\varepsilon_\Pi u(d)+\left[2\int_{\mathbb{R}^2\setminus S_2} dAu(r_2)\right.\\ &\left.-\frac{1}{2}\pi r_{0,\mathrm{ref}}^3\left(\varepsilon_\Pi-\frac{2u_0}{r_{0,\mathrm{ref}}}\right)\right]\Pi(d)+\cdots,\end{aligned} \tag{43}$$

where we have employed Eq. (28) (with $\lambda^{-1}=0$ for simplicity). Convergence of the integral of u imposes the more stringent constraint $n>4$ on the decay of Π [see Eq. (42)].

The validity of formulas (40) and (43) has been checked explicitly by comparing their predictions with the numerical evaluation of the integral for a surface stress of the form $\Pi \propto r^{-n}$ with $n>4$.

(2) The second term in Eq. (39) can be estimated in the limit $d\to\infty$ by expanding the integrand into a Taylor series, which is uniformly valid in the integration domain

$$\begin{aligned}\int_{S_1} dA\Pi_2 u_2 \simeq& \int_{S_1} dA[\Pi_2 u_2+\cdots]_{\mathbf{r}_2=d\mathbf{e}_x}\\ \simeq& \pi r_{0,\mathrm{ref}}^2\Pi(d)u(d)+\cdots.\end{aligned} \tag{44}$$

(3) The third term in Eq. (39) reads

$$\oint_{\partial S_1} d\ell\frac{\partial(u_1u_2)}{\partial n_1}=\int_0^{2\pi}d\varphi[\mathbf{r}_1\cdot\boldsymbol{\nabla}(u_1u_2)]_{r_1=r_{0,\mathrm{ref}}}\simeq\int_0^{2\pi}d\varphi\left((\mathbf{r}_1\cdot\boldsymbol{\nabla})\left\{u_1\left[u_2+\mathbf{r}_1\cdot(\boldsymbol{\nabla}u)_2+\frac{1}{2}\mathbf{r}_1\mathbf{r}_1:(\boldsymbol{\nabla}\boldsymbol{\nabla}u)_2+\cdots\right]_{\mathbf{r}_2=d\mathbf{e}_x}\right\}\right)_{r_1=r_{0,\mathrm{ref}}} \tag{45}$$

$$\simeq 2\pi r_{0,\mathrm{ref}}u(d)\left.\frac{du}{dr}\right|_{r=r_{0,\mathrm{ref}}}+\frac{\pi}{2}r_{0,\mathrm{ref}}\boldsymbol{\nabla}^2u(d)\left.\frac{d(r^2u)}{dr}\right|_{r=r_{0,\mathrm{ref}}}+\cdots\simeq 2\pi r_{0,\mathrm{ref}}\varepsilon_F u(d)-\frac{\pi}{2\gamma}r_{0,\mathrm{ref}}^3\left(\varepsilon_F+\frac{2u_0}{r_{0,\mathrm{ref}}}\right)\Pi(d)+\cdots \tag{46}$$

using the boundary condition for u in Eq. (17).

(4) The fourth term in Eq. (39) is evaluated analogously:

$$\oint_{\partial S_1} d\ell \frac{\partial u_2^2}{\partial n_1} = \int_0^{2\pi} d\varphi [\mathbf{r}_1 \cdot \boldsymbol{\nabla} u_2^2]_{r_1=r_{0,\mathrm{ref}}} \tag{47}$$

$$\simeq \int_0^{2\pi} d\varphi \{\mathbf{r}_1 \cdot [(\boldsymbol{\nabla} u^2)_2 + \mathbf{r}_1 \cdot (\boldsymbol{\nabla}\boldsymbol{\nabla} u^2)_2 + \cdots]_{\mathbf{r}_2=d\mathbf{e}_x}\}_{r_1=r_{0,\mathrm{ref}}}$$

$$\simeq \pi r_{0,\mathrm{ref}}^2 \boldsymbol{\nabla}^2 u^2(d) + \cdots . \tag{48}$$

(5) The fifth term in Eq. (39) is given by

$$\frac{1}{r_{0,\mathrm{ref}}} \oint_{\partial S_1} d\ell [u_2 - \overline{u}]^2 = \int_0^{2\pi} d\varphi u_2^2 - 2\pi \overline{u}^2$$

$$\simeq \tfrac{1}{2}\pi r_{0,\mathrm{ref}}^2 [\boldsymbol{\nabla}^2 u^2(d) - 2u\boldsymbol{\nabla}^2 u(d)] + \cdots$$

$$\simeq \tfrac{1}{2}\pi r_{0,\mathrm{ref}}^2 \left[\boldsymbol{\nabla}^2 u^2(d) + \frac{2}{\gamma}\Pi(d) u(d) \right] + \cdots . \tag{49}$$

(6) In order to evaluate the sixth term in Eq. (39), we expand u_2 in the definition given by Eq. (35):

$$\overline{u} = \frac{1}{2\pi r_{0,\mathrm{ref}}} \oint_{\partial S_1} d\ell u_2$$

$$\simeq u(d) + \frac{1}{4} r_{0,\mathrm{ref}}^2 \boldsymbol{\nabla}^2 u(d) + \cdots$$

$$\simeq u(d) - \frac{1}{4\gamma} r_{0,\mathrm{ref}}^2 \Pi(d) + \cdots . \tag{50}$$

The asymptotic behavior of the effective potential is finally obtained from Eq. (39) by collecting all terms. There are two qualitatively different cases.

$\varepsilon_\Pi \neq \varepsilon_F$: The limit $\lambda \to \infty$ is singular and the single-colloid meniscus profile exhibits a logarithmic dependence. One finds that the leading contribution is provided by the terms proportional to $u(d)$:

$$V_{\mathrm{men}}(d) \simeq 2\pi\gamma r_{0,\mathrm{ref}} (\varepsilon_F - \varepsilon_\Pi) u(d)$$

$$\simeq -2\pi\gamma r_{0,\mathrm{ref}}^2 (\varepsilon_F - \varepsilon_\Pi)^2 \ln \frac{C\lambda}{d}, \quad (R \ll d \ll \lambda), \tag{51}$$

which represents a long-ranged attractive effective potential, irrespective of the sign of the forces F and Π acting on the system.

$\varepsilon_\Pi = \varepsilon_F$: The single-colloid meniscus profile decays like $u(d) \sim d^{2-n}$ if $\Pi(d) \sim d^{-n}$. The leading contribution is proportional to $\Pi(d)$, because the terms proportional to $u(d)$ cancel each other.

$$V_{\mathrm{men}}(d) \simeq -2\Pi(d) \int_{\mathbb{R}^2 \setminus S} dA u, \quad (R \ll d \ll \lambda). \tag{52}$$

This correspond to a shorter-ranged effective interaction, which in principle can be either attractive or repulsive depending on the precise form of the function $\Pi(r)$. In the particular case that $\Pi(r)$ decays monotonically to zero, e.g., $\Pi(r) \propto r^{-n}$, it is easy to check that V_{men} amounts to a repulsive force, because the sign of u is opposite to the sign of Π.

We have seen that the error committed by the superposition approximation in satisfying one of the boundary conditions, Eq. (33), decays like $\Pi(d)$, too. This suggests that the corrections to the superposition approximation could modify the precise value of the constant factor acting as an amplitude in Eq. (52), and *a priori* it cannot be excluded that there are cancellations leading to a vanishing amplitude, and therefore to an even faster decay for large d. Thus the superposition approximation might not be reliable enough for calculating V_{men} if $\varepsilon_\Pi = \varepsilon_F$.

If one traces back the origin of the dominant contributions to V_{men}, one finds that in both cases only the first, third, and sixth term in Eq. (39) are relevant. They correspond physically to the effect of the overlap of the two single-colloid meniscus profiles and the change of the colloid height [first integral and the term $-2F\overline{u}$ in Eq. (37), respectively].

IV. APPLICATIONS AND DISCUSSION

Equations (51) and (52) describe the asymptotic behavior of the meniscus-induced effective intercolloidal potential and thus represent a central result of our analysis. They provide the explicit functional dependence on an arbitrary stress field $\Pi(r)$ which decays sufficiently fast. The assumptions entering their derivation are (i) that the deviations of the meniscus profile from the reference configuration are small, allowing one to confine the analysis to a free energy expression which is quadratic in the deviations, and (ii) the superposition approximation, which expresses the two-colloid equilibrium state in terms of the single-colloid state. The analysis shows that the limit $\lambda \to +\infty$ is nonsingular only in the case $\varepsilon_F = \varepsilon_\Pi$.

A. Flotation force

Equation (51) can be used to determine the flotation force. There are no stresses acting at the meniscus, $\Pi \equiv 0$, while the force F on the colloids is due to their weight corrected by the buoyancy force. Accordingly, Eq. (51) reduces to the flotation potential

$$V_{\mathrm{flot}}(d) = 2\pi\gamma r_{0,\mathrm{ref}} \varepsilon_F u(d) = 2\pi\gamma Q^2 \ln \frac{d}{C\lambda}, \quad (R \ll d \ll \lambda), \tag{53}$$

where $Q := \varepsilon_F r_{0,\mathrm{ref}}$ is known as the capillary charge [17], by analogy with two-dimensional electrostatics. The asymptotic form for $d \ll \lambda$ originates from a potential proportional to the modified Bessel function $K_0(d/\lambda)$ [see Eq. (19)] [24,26]. The order of magnitude of the capillary charge is Q

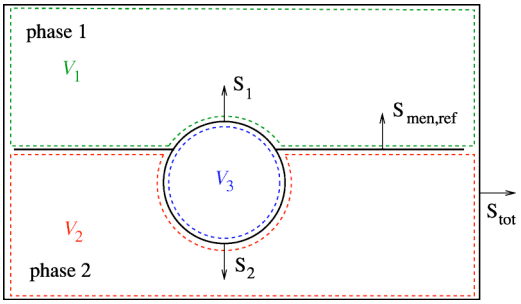

FIG. 6. (Color online) In the reference configuration the whole system is divided into volumes V_1, V_2, and V_3. Volume V_1 (enclosed by the upper dashed curve) includes phase 1, volume V_2 (enclosed by the lower dashed curve) includes phase 2, and volume V_3 includes the interior of the colloid. The arrows indicate the direction in which the surfaces (including the infinitesimally displaced ones) are oriented: S_{tot} encloses the whole system, $S_{men,ref}$ is the interface between phase 1 and phase 2, and $S_{1(2)}$ denotes the interface between the colloid and phase 1(2).

$\sim r_{0,ref}(R/\lambda)^2$. For a typical value $\gamma=0.05$ N m^{-1} at room temperature and for colloids with a mass density of the order of 1 g cm^{-3}, the prefactor of the logarithm can be estimated as

$$2\pi\gamma Q^2 \sim \left(\frac{R}{10\ \mu\text{m}}\right)^6 k_B T. \tag{54}$$

Therefore, compared with the thermal energy, the flotation force is negligible for submicrometer-sized colloids.

B. Electrically charged colloids

Another application is the case of electrically charged colloids. If one of the liquid phases is water, the charge of the colloid is screened (the Debye length of pure water is $\approx 1\ \mu$m and smaller in the presence of an electrolyte), and the effective electric field is that of a dipole oriented perpendicularly to the fluid interface [4,5,27–29]. The electrostatic field decays as r^{-3} and the stress on the meniscus as $\Pi(r \to \infty) \propto r^{-6}$. Both the electrostatic stress and the osmotic ionic pressure decay in the same manner [15]. Thus the total intercolloidal potential at intermediate distances is

$$V_{tot} = a\frac{k_B T}{d^3} + V_{men} \quad (a > 0). \tag{55}$$

If gravity is neglected both as a force on the colloid and as a restoring force for the interface ($\lambda \to \infty$), then one can indeed show that the ensuing condition of mechanical isolation (no net force on the system) leads to $\varepsilon_\Pi = \varepsilon_F$, i.e., precisely the situation for which the limit $\lambda \to \infty$ is nonsingular. To see this, we consider the total stress tensor $\mathbf{T}$ which consists of the Maxwell stress tensor (due to the electrostatic field) and a diagonal osmotic pressure tensor (due to the electrolytes) [18,30]. At interfaces $\mathbf{T}$ can be discontinuous. The total volume V of the system is divided into volumes V_1, V_2, and V_3 (see Fig. 6 for the explanation of the notation in the following equation). The total force reads [the superscript $^{+(-)}$ denotes evaluation on the positive(negative) side of the oriented surface, i.e., the side the arrows in Fig. 6 point to (do not point to)]

$$\begin{aligned}
\oint_{S_{tot}} d\mathbf{A}\cdot\mathbf{T} &= \int_{V_1\cup V_2\cup V_3} dV(\boldsymbol{\nabla}\cdot\mathbf{T}) \\
&\quad + \int_{S_{men,ref}\cup S_1\cup S_2} d\mathbf{A}\cdot(\mathbf{T}^+ - \mathbf{T}^-) \\
&= \int_{V_1\cup V_2} dV(\boldsymbol{\nabla}\cdot\mathbf{T}) + \int_{S_{men,ref}} d\mathbf{A}\cdot(\mathbf{T}^+ - \mathbf{T}^-) \\
&\quad + \left[\int_{V_3} dV(\boldsymbol{\nabla}\cdot\mathbf{T}) + \int_{S_1\cup S_2} d\mathbf{A}\cdot(\mathbf{T}^+ - \mathbf{T}^-)\right] \\
&= \int_{S_{men,ref}} dA\Pi\mathbf{e}_z + F\mathbf{e}_z.
\end{aligned} \tag{56}$$

In the first line, we have applied Gauss' theorem with due account of the possible discontinuities of the tensor $\mathbf{T}$ across the interfaces. In the second line, $\boldsymbol{\nabla}\cdot\mathbf{T}=0$ in the fluid phases V_1 and V_2, because the counterion distribution of the reference configuration is the equilibrium distribution and thus locally force free. This distribution is considered to be fixed. The second term in the second line is the total force on the meniscus (which can have only a normal component), while the terms in square brackets sum up to the force F acting on the colloid.

Thus the vertical component of the total force is

$$\mathbf{e}_z\cdot\oint_{S_{tot}} d\mathbf{A}\cdot\mathbf{T} = 2\pi\gamma r_{0,ref}(\varepsilon_\Pi - \varepsilon_F). \tag{57}$$

If it vanishes, as it is the case for an isolated system, then $\varepsilon_\Pi = \varepsilon_F$. According to Eq. (51) this implies that the long-ranged logarithmic contribution to V_{men} is absent and thus the limit $\lambda \to \infty$ is regular. Physically this means that there is no need for a restoring force acting on the fluid-fluid interface when the deformation is created by localized internal stresses. Instead, according to Eq. (52), one obtains a potential $V_{men} \propto d^{-6}$ for the present case of a dipolar electric field (see above). This shorter-ranged potential cannot counterbalance the direct electrostatic dipolar repulsion $\sim d^{-3}$. Such a counterbalance would be needed for a straightforward explanation of the aforementioned experimentally observed attractions.

The line of argument to explain the absence of the logarithmic contribution to V_{men} was already put forward in Refs. [13,15], where exclusively the case $\Pi(r) \propto r^{-6}$ has been addressed. Our detailed analysis complements and generalizes these contributions. In Ref. [13], $V_{men}(d)$ is estimated by taking into account only the degree of freedom "meniscus profile," $u(\mathbf{r})$, and considering only the change in meniscus area due to the superposition of the dimples. This corresponds to retaining only the term $\propto(\boldsymbol{\nabla}u_1)\cdot(\boldsymbol{\nabla}u_2)$ in expression (37). Although the type of d dependence obtained that way is correct, the sign of the force turns out to be wrong (attraction instead of repulsion). The reason is that the contributions $\propto\Pi_1 u_2$ and $\propto F\overline{u}$ in Eq. (37) are equally important as the retained term. This is taken into account in the more detailed

analysis of Ref. [15], where the limiting case $R=0$ (point particle) is considered from the outset, so that "height of the colloid" is not an independent degree of freedom, i.e., $h=u(0)$. Correspondingly, F is set to zero ($\varepsilon_F=0$), and its effect is modelled by a Dirac δ contribution to the stress $\Pi(r)$ such that $\varepsilon_\Pi=0$. The potential $V_{\mathrm{men}}(d)$ calculated this way corresponds to keeping the three terms mentioned above which are relevant [the first and third term in the first integral of Eq. (37) and the last term of Eq. (37)] and to setting $\lambda\to\infty$, since this limit is regular when $\varepsilon_F=\varepsilon_\Pi=0$. Our analysis has shown that the terms which are dropped in the limit $R\to 0$ [second and third integral in Eq. (37), second, fourth, and fifth terms in Eq. (39)] yield indeed a subdominant contribution to Eq. (52). However, the integral appearing as a prefactor in Eq. (52) is divergent for $R\to 0$, so that in Ref. [15] a short-distance cutoff a has been introduced which is expected to be of the order of R. The precise value of a depends on the details of the implementation of this cutoff; for the example used in Ref. [15], the application of Eq. (52) yields $a=r_{0,\mathrm{ref}}$.

In the presence of gravity mechanical isolation is violated and as we have shown $|\varepsilon_\Pi-\varepsilon_F|\propto(R/\lambda)^2$. **(**The force-balance argument [Eq. (56)] can be easily generalized to include the effect of the gravitational volume force.**)** In the case of a curved reference interface (corresponding to the experiment reported in Ref. [12] using colloids trapped at the interface of water droplets in oil), Eq. (56) is replaced by

$$\oint_{S_{\mathrm{tot}}} d\mathbf{A}\cdot\mathbf{T}=\int_{S_{\mathrm{men,ref}}} dA\Pi\mathbf{e}_r+F\mathbf{e}_z, \tag{58}$$

where $\mathbf{e}_r$ is the radial unit vector of the unperturbed spherical droplet. Force balance in the vertical direction yields a factor $\mathbf{e}_r\cdot\mathbf{e}_z=\cos\psi$ (see Fig. 4) in the integral, which can be expanded for small angles in the limit $R_{\mathrm{drop}}\to\infty$. This leads to a curvature-induced correction $|\varepsilon_\Pi-\varepsilon_F|\propto(r_{0,\mathrm{ref}}/R_{\mathrm{drop}})^2$ even for mechanical isolation. Thus we see that independently of the details of the implementation of the distant boundary conditions the logarithmic term in the potential V_{men} [Eq. (51)] has a strength which is proportional to (colloid size/system length)^4, which seems nevertheless too weak to explain the reported attractive total interaction.

1. The experiment reported in Ref. [12]

Mechanical isolation is violated in the presence of an external homogeneous electric field $E\mathbf{e}_z$. For the experimental setup used in Ref. [12] it cannot be ruled out that such an external field may have distorted the measurements [31]. Since this is the only experiment which provides quantitative information about the secondary minimum in V_{tot}, we discuss the case of an external field in more detail. In this experiment position-recording measurements were performed on a hexagonal configuration of seven trapped colloids on a water droplet immersed in oil ($R_{\mathrm{drop}}\approx 32R=24\ \mu$m). The latter was confined between two glass plates and the droplet stuck on the upper glass plate with a contact angle close to π. Residual charges might have resided on the upper plate [31]. The measurements yielded the position of the secondary minimum, $d_{\mathrm{min}}\approx 7.6R$, and the curvature at the minimum, $V''_{\mathrm{tot}}(d_{\mathrm{min}})\approx 12.94k_BT/R^2$. With regard to the latter value we remark that systematic corrections can be estimated to lower V''_{tot} by a factor 2–3. These systematic corrections include (i) multiparticle effects and (ii) center-of-mass movement of the droplet. We have estimated the effect of (i) by carrying out Langevin simulations of the seven particle system using the intercolloidal potential Eq. (59) below. As for the effect of (ii), any shape deformation induced by the moving colloids changes the center-of-mass position of the droplet since the droplet is fixed to the upper glass plate. The corresponding change in the gravitational energy of the droplet translates into a weak confining potential for the colloids which limits the stochastic movement of the center-of-mass of the seven colloids. This effect might be part of an explanation for the absence of center-of-mass movement observed in Ref. [12]. According to Eqs. (51) and (55), the total intercolloidal potential in an external field is

$$V_{\mathrm{tot}}=a\frac{k_BT}{d^3}-b\ln\frac{C\lambda}{d}\quad(a,b>0). \tag{59}$$

Using the aforementioned experimental data for d_{min} and $V''_{\mathrm{tot}}(d_{\mathrm{min}})$, one obtains from Eq. (59) $b\approx 249k_BT$, $a\approx 83d_{\mathrm{min}}^3$ and $V_{\mathrm{tot}}(d_{\mathrm{min}})\approx -275k_BT$ which is surprisingly deep, even if reduced by a factor 2–3 due to the systematic corrections mentioned above. Furthermore, from Eq. (51) we deduce $b=2\pi\gamma r_{0,\mathrm{ref}}^2(\varepsilon_\Pi-\varepsilon_F)^2$ and with $\gamma\approx 0.05$ N/m we find $|\varepsilon_\Pi-\varepsilon_F|\approx(2\ \mathrm{nm}/r_{0,\mathrm{ref}})$. The long-ranged meniscus deformation [see Eq. (20)] is on the scale of nanometers. The short-ranged meniscus deformation near the colloid can only be evaluated with a specific microscopic model for $\Pi(r)$. For a rough estimate of ε_Π, we consider the colloid charge to be concentrated on the surface. The asymptotic behavior of the stress tensor in this case is given by $\Pi(r)=(ak_BT)/(4\pi r^6)$ [4,15]. If we assume this form of the stress tensor to hold for all r, we find $\varepsilon_\Pi\approx 10^{-4}/\sin^5\theta$ for the values of γ and a given above. For not too small contact angles, this *a posteriori* justifies the perturbative approach which we have adopted.

If the system has a net charge q, then $|qE|=2\pi\gamma r_{0,\mathrm{ref}}|\varepsilon_\Pi-\varepsilon_F|=\sqrt{2\pi\gamma b}$ [see Eqs. (57) and (51)]. Using the values for b and γ as given above we find

$$|qE|\approx 3.6\times 10^9\ \mathrm{eV\ m^{-1}}. \tag{60}$$

For the value $q\approx 2\times 10^5$ e quoted in Ref. [12], this yields a relatively small electric field $E\approx 1.8\times 10^4$ V m^{-1}, indicating how sensitive the system can be to spurious external fields. Alternatively, an electric field $E\sim 10^3$ V m^{-1} is sufficient for the meniscus-induced logarithmic potential to have a depth of the order $b\sim 1k_BT$. Thus the external field offers the possibility to tune easily the capillary long-ranged attraction and to manipulate the structures formed by the colloids at the interface.

2. The experiment and analysis reported in Ref. [16]

In Ref. [16], experimental results for the meniscus deformation around glass particles of radii $200\cdots 300\ \mu$m trapped at water-air or water-oil interfaces are reported. The data for the meniscus slope $u'(r_0)$ at the contact circle imply [Eq. (17)] $\varepsilon_F\approx 0.2$ (water-oil interface), about fifteen times larger

than the corresponding $\varepsilon_{F,\mathrm{g}}$ caused by gravity alone. Furthermore, the reported meniscus shape for one sample contains a logarithmic part which is consistent with $\varepsilon_F - \varepsilon_\Pi \approx 0.1 \gg \varepsilon_{F,\mathrm{g}}$ [see Eq. (20)]. As in the experiment analyzed in the previous subsection, the experimental observations could be understood within the framework of the theoretical model we have developed in terms of an external electric field violating mechanical isolation. Yet independently of us, the authors of Ref. [16] have developed a theoretical model based on the same physical hypotheses as our approach which, they claim, explains the observed long-ranged meniscus deformation. Here we would like to note two important errors which flaw their analysis.

(1) Eq. (3.15) in Ref. [16], in terms of which they interpret their observations, can be obtained by inserting the large-distance ($r \gg r_{0,\mathrm{ref}}$) asymptotic behavior of $\Pi(r)$ in our Eq. (20) [equivalent to their Eq. (3.14) up to an additive constant] both into the integral term *and into the definition of* ε_Π [Eq. (2)]. Since the dominant contribution to the integral defining ε_Π stems from points $r \simeq r_{0,\mathrm{ref}}$, this procedure is clearly inadmissible. As a consequence, they obtain a wrong, nonvanishing prefactor of the logarithm, in spite of their explicit consideration of mechanical isolation [see their Eq. (6.6)].

(2) In order to calculate the intercolloidal effective potential within the superposition approximation, the formula relating $V_{\mathrm{men}}(d)$ to the meniscus deformation $u(d)$ *in the presence of gravity alone* [i.e., Eq. (53)] is applied even though $\Pi \neq 0$. Thus, an additional term contributing to the leading logarithm is not included [compare their Eq. (3.16) and our Eq. (51)].

In Ref. [16] also a numerical analysis is carried out. A detailed study of the relation between the results of this numerical analysis and our theoretical predictions will be published elsewhere.

It may be possible that the presence of an external field is consistent with the data from Refs. [12,16], as well as with the presence of the secondary potential minimum observed in the experiments using planar troughs, in particular in the cases $d_{\min} > 10R$, which fall into the intermediate asymptotic regime considered here. But this still remains as an open problem.

C. Outlook

Given that already nanometer distortions of the meniscus produce noticeable attractions, the surface topography of colloids might be relevant. In Ref. [10], colloidal surface roughness is proposed as an explanation of the attraction. The meniscus contact line is assumed to be pinned at defects on the colloid surface caused by surface roughness. This imposes a different boundary condition for the meniscus at contact, which is then deformed even in the absence of electrostatic forces. The corresponding analysis in Ref. [10] is concerned only with the term $\propto(\boldsymbol{\nabla} u_1)\cdot(\boldsymbol{\nabla} u_2)$ in the expression (37), leading to the conclusion that $V_{\mathrm{men}}(d)$ decays as d^{-4} and corresponds to an attractive potential with a strength of $10^4\ k_BT$ for meniscus deformations of the order of 50 nm. This conclusion, however, cannot be simply carried over to the case of charged colloids. As we have shown the contributions of the terms $\propto \Pi_1 u_2$ and $\propto F\overline{u}$ in Eq. (37) are relevant and can change the qualitative behavior of $V_{\mathrm{men}}(d)$ even in the limit of point colloids. It would be worthwhile to generalize the analysis of Ref. [10] along the line of arguments presented here in order to assess the importance of surface roughness. This should be complemented by more precise experimental information about the actual colloidal topography.

Recently, an explanation based on a contaminated interface has been advocated [32]. The air-water interface would be actually a two-dimensional emulsion consisting of hydrophylic (water) patches and hydrophobic (silicon oil) patches. The colloidal particles (hydrophobic in character according to Ref. [32]) would cluster in the hydrophobic patches. Thus, confinement of the colloids by finite-size hydrophobic patches would give the impression of an effective intercolloidal attraction. At present, this explanation is only of qualitative nature.

Thermal fluctuations of the interface position around its mean value $u(\mathbf{r})$ also induce an effective interaction between the colloids which confine these fluctuations (Casimir-like force). Using a Gaussian model of the fluctuating interface in analogy to the procedure employed in Ref. [33] for calculating fluctuation-induced forces between rods in a membrane, one finds for uncharged colloids a fluctuation-induced potential $V_{\mathrm{fluc}} \simeq -k_BT(r_{0,\mathrm{ref}}/d)^4$, which is too small and falls off more rapidly than the intercolloidal dipole repulsion. Here, the generalization to the charged case might give hints for the effective attractions between *very* small particles trapped at interfaces. Concerning particle sizes well below the Debye length, one should modify our analysis to account for the overlap of the screening ionic clouds [this would affect, e.g., the superposition approximation for the stress field Π, Eq. (31)].

Finally, in Ref. [34] the attraction of particles trapped at a nematic-air interface is reported and an explanation in terms of a logarithmic meniscus deformation is proposed which parallels the explanation given in Ref. [12]: in this case, the deformation would be caused by the elastic distortion induced by the particles on the nematic phase [34]. Our detailed theoretical treatment shows that no long-range (logarithmic) meniscus distortion can arise on an interface if the system is mechanically isolated and the excess free energy of the perturbed interface is correctly described by an expression like Eq. (13). Thus it appears that the simple explanation of the observed colloidal attractions given in Ref. [34] is not correct. However, it is not clear whether the free energy of a distorted nematic-air interface is equivalent to that of a simple fluid interface due to the long-ranged interactions in the nematic bulk caused by defects. Thus, a generalization of our theory to interfaces involving nematic phases would be desirable in order to assess the possibility of long-ranged colloidal attractions in more detail.

V. SUMMARY

We have analyzed the effective force induced by capillary deformation between two smooth spherical colloids floating

at a fluid interface. The relevant degrees of freedom are the meniscus deformation and the height of the colloids (Fig. 2), whose equilibrium values are given by minimization of a free energy functional. This functional was derived assuming small deviations from a reference configuration (Fig. 1). It incorporates the surface tensions of the three interfaces involved ("colloid-fluid phase 1," "colloid-fluid phase 2," and "fluid phase 1-fluid phase 2"), the potential energy of the colloids under the action of a force F, the potential energy of the fluid interface in an arbitrary surface stress field $\Pi(\mathbf{r})$, and the potential energy due to a restoring force acting on the interface [Eqs. (4)–(13)]. The effective intercolloidal potential [Eq. (36)] was calculated in the limit of large separations by using the superposition approximation [Eq. (31)]. We have shown in this limit that the contribution to the effective potential by the interfaces colloid-fluid phases is subdominant. If the total force acting on the system, consisting of the two colloids and the meniscus, does not vanish, the presence of the restoring force acting on the fluid interface is essential—although its precise form does not matter (Sec. II C). In this case, the effective interaction is long-ranged and attractive [Eq. (51)]. If the total force vanishes, the restoring force is irrelevant altogether, the effective interaction is shorter ranged [Eq. (52)], and it cannot be computed reliably within the superposition approximation.

As an application, we have considered the case of like-charged, micrometer-sized particles when the capillary deformation is due to the ensuing electrostatic field. We have discussed how one can tune the long-ranged attractive interaction by an external electric field, but we conclude that the experimentally observed attraction in an isolated system cannot be explained within the present model. Possible directions for future research such as colloidal surface roughness and fluctuations of the interface have been discussed.

ACKNOWLEDGMENTS

We kindly acknowledge helpful discussions on the subject of the manuscript with M. Nikolaides, A. Bausch, K. Danov, and P. Kralchevsky.

APPENDIX A: FREE ENERGY OF COLLOID-FLUID CONTACT

In this appendix we determine the contribution to the free energy due to the exposure of the colloid to the two fluid phases. Here we consider the general case of no rotational invariance, so that the meniscus height $u(r,\varphi)$ depends on the distance r from the axis through the colloid center and on the angle of revolution φ around this axis (Fig. 7). Accordingly, the auxiliary variables $r_0(\varphi)$ and $\xi(\varphi)$ also depend on the revolution angle and one has

$$r_0(\varphi) = R \sin \xi(\varphi) \tag{A1}$$

and

$$h = u(r_0(\varphi),\varphi) - R\cos\xi(\varphi), \tag{A2}$$

where $u(r_0(\varphi),\varphi)$ is the meniscus height at contact. The surface areas of the colloid in contact with phases 1 and 2 are

$$A_1 = R^2\int_0^{2\pi} d\varphi \int_0^{\xi(\varphi)} d\psi \sin\psi = R^2\int_0^{2\pi} d\varphi[1-\cos\xi(\varphi)] \tag{A3}$$

and

$$A_2 = 4\pi R^2 - A_1, \tag{A4}$$

respectively. The expression for the free energy in Eq. (5) is based on these formulas for the special case $\xi_{\mathrm{ref}}(\varphi)=\theta$ (Fig. 1) and on Young's law [Eq. (1)]:

$$\begin{aligned}\mathcal{F}_{\mathrm{cont}} &= \gamma R^2\int_0^{2\pi} d\varphi[\cos^2\theta - \cos\theta\cos\xi(\varphi)] \\ &= \tfrac{1}{2}\gamma R^2\int_0^{2\pi} d\varphi[\cos\xi(\varphi)-\cos\theta]^2 \\ &\quad + \tfrac{1}{2}\gamma R^2\int_0^{2\pi} d\varphi[\cos^2\theta - \cos^2\xi(\varphi)] \\ &= \tfrac{1}{2}\gamma\int_0^{2\pi} d\varphi\{u(r_0(\varphi),\varphi)-\Delta h\}^2 \\ &\quad + \tfrac{1}{2}\gamma\int_0^{2\pi} d\varphi[r_0^2(\varphi) - r_{0,\mathrm{ref}}^2].\end{aligned} \tag{A5}$$

The second term, which arises upon completing the square, represents the change of the meniscus area which is cut out by the colloid. Since u and Δh are already of first order in ε_Π or ε_F, one can replace $r_0(\varphi)$ by $r_{0,\mathrm{ref}}$ in the first term and obtains

$$\begin{aligned}\mathcal{F}_{\mathrm{cont}} &\simeq \tfrac{1}{2}\gamma\int_0^{2\pi} d\varphi[u(r_{0,\mathrm{ref}},\varphi)-\Delta h]^2 \\ &\quad + \tfrac{1}{2}\gamma\int_0^{2\pi} d\varphi[r_0^2(\varphi) - r_{0,\mathrm{ref}}^2],\end{aligned} \tag{A6}$$

plus corrections of at least third order in ε_Π or ε_F. In the special case of rotational invariance, this expression reduces to Eq. (6). For the purpose of Sec. III one can rewrite Eq. (A6) as the line integral

$$\mathcal{F}_{\mathrm{cont}} \simeq \frac{\gamma}{2r_{0,\mathrm{ref}}}\oint_{\partial S} d\ell\{[u-\Delta h]^2 + [r_0^2 - r_{0,\mathrm{ref}}^2]\}, \tag{A7}$$

where S is a circular disk of radius $r_{0,\mathrm{ref}}$, here centered at the origin, and ∂S denotes its circumference.

APPENDIX B: DEFORMATION OF A SPHERICAL REFERENCE INTERFACE

In this appendix we calculate the deformation of the interface of a spherical droplet due to a floating colloidal particle. The reference configuration corresponds to a colloid

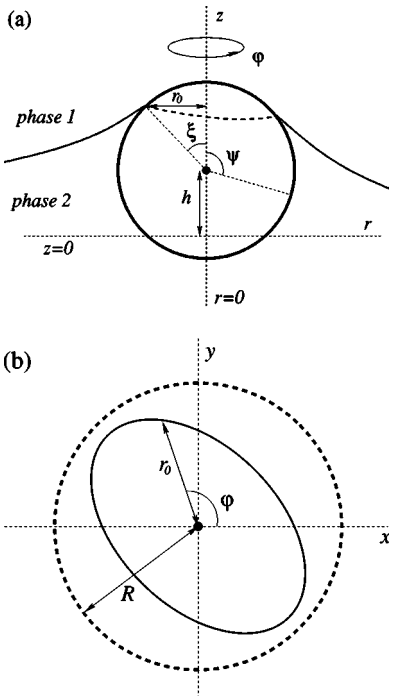

FIG. 7. Geometric description of the three-phase contact line between the fluid-fluid interface and the surface of the colloid. Side view (a): The auxiliary variables $r_0(\varphi)$ and $\xi(\varphi)$ in general depend on the angle of revolution φ. ψ denotes the polar angle of points on the colloid spherical surface. Top view (b): The dashed line is the circumference of radius R of the spherical colloid. The solid line is the projection of a noncircular contact line.

floating at the surface of the spherical droplet such that Eq. (1) is fulfilled. Here we will consider only axially symmetric configurations (see Fig. 4). In terms of the polar angle $\psi \in [0,\pi]$, the distance r measured along the unperturbed spherical droplet surface is $r=R_{\mathrm{drop}}\psi$. [Note that in this appendix we consider $u(\cdot)$ and $\Pi(\cdot)$ as functions of ψ instead of r.] We define $\psi_0 := r_{0,\mathrm{ref}}/R_{\mathrm{drop}}$ and we introduce the angle ψ_1 with $\pi > \psi_1 \gg \psi_0$ at which another boundary condition (to be specified below) holds reflecting the fact that the droplet is fixed in space. With this additional boundary condition we model closely the actual experimental setup of Ref. [12], where the droplet was attached to a glass plate with a contact angle less than π [31].

For the present case the free energy given by Eq. (13) must be modified in several ways:

In spherical coordinates, $\mathcal{F}_{\mathrm{men}}$ reads

$$\mathcal{F}_{\mathrm{men}} = \gamma \int_{S_{\mathrm{men}}} dA (R_{\mathrm{drop}}+u)^2 \sqrt{1+\left|\frac{\boldsymbol{\nabla} u}{R_{\mathrm{drop}}+u}\right|^2} - \gamma \int_{S_{\mathrm{men,ref}}} dA R_{\mathrm{drop}}^2, \tag{B1}$$

where $dA = 2\pi \sin\psi d\psi$ is the differential of the solid angle, and $\boldsymbol{\nabla} = \mathbf{e}_\psi (d/d\psi)$ is the gradient operator on the unit sphere. As before, this functional is now expanded for small deviations from the reference configuration, and we obtain

$$\mathcal{F}_{\mathrm{men}} \simeq \gamma\pi (r_{0,\mathrm{ref}}^2 - r_0^2) + 2\pi\gamma \int_{\psi_0}^{\psi_1} d\psi \times \sin\psi \left[\frac{1}{2}\left(\frac{du}{d\psi}\right)^2 + u^2 + 2R_{\mathrm{drop}} u \right], \tag{B2}$$

where we have neglected terms evaluated at ψ_0 which vanish in the limit $R_{\mathrm{drop}} \to \infty$.

The term $\mathcal{F}_{\mathrm{inter}}$ in Eq. (11) has to be amended by the extra work upon deformation which is caused by the pressure difference in the reference configuration between the interior and the exterior of the droplet, $\Delta P = 2\gamma/R_{\mathrm{drop}}$:

$$\mathcal{F}_{\mathrm{inter}} = -\int_{S_{\mathrm{men}}} dA \left[R_{\mathrm{drop}}^2 \Pi u + (\Delta P) \int_0^u d\tilde{u} (R_{\mathrm{drop}} + \tilde{u})^2 \right] \simeq -2\pi\gamma \int_{\psi_0}^{\psi_1} d\psi \sin\psi \left[\frac{R_{\mathrm{drop}}^2}{\gamma} \Pi u + (2R_{\mathrm{drop}} u + 2u^2) \right]. \tag{B3}$$

Since ΔP is of order ε^0, we have to keep also terms $\propto u^2$ in this expression for consistency. For simplicity we have neglected the contribution due to the change of S_{men} during the deformation. Such a term would affect the behavior of the meniscus only near ψ_0 and vanishes in the limit $R_{\mathrm{drop}} \to \infty$.

The change in volume of the perturbed droplet reads

$$\Delta V = \int_{S_{\mathrm{men}}} dA \tfrac{1}{3}(R_{\mathrm{drop}}+u)^3 - \int_{S_{\mathrm{men,ref}}} dA \tfrac{1}{3} R_{\mathrm{drop}}^3 + \delta, \tag{B4}$$

where δ is a contribution due to the spherical shape of the colloid; it depends on Δh and Δr_0 but can be safely neglected. [This is the same kind of term encountered in calculating $\mathcal{F}_{\mathrm{vol}}$, see Eq. (10).] Expanding ΔV for small deformations u up to linear order yields

$$\Delta V \simeq 2\pi R_{\mathrm{drop}}^2 \int_{\psi_0}^{\psi_1} d\psi \sin\psi u. \tag{B5}$$

Physically, the deformation of the interface occurs under the constraint that the droplet volume remains unchanged because incompressibility is assumed. This constraint ($\Delta V = 0$) will be implemented in the free energy functional by means of a Lagrange multiplier μ which itself turns out to be linear in the parameters ε_Π and ε_F. This justifies keeping only the linear term in Eq. (B5).

The contribution $\mathcal{F}_{\mathrm{cont}}$ [see Eq. (6)] is concerned only with quantities at ψ_0, the colloid surface, and thus in the limit of large droplet radii this contribution is the same as in the planar case. The free energy related to the work done upon moving the colloid, $\mathcal{F}_{\mathrm{coll}}$ [see Eq. (12)], remains also unchanged. For simplicity we also neglect gravity and set $\lambda^{-1} = 0$. In conclusion, the free energy functional to be minimized is the sum $\mathcal{F}_{\mathrm{cont}} + \mathcal{F}_{\mathrm{men}} + \mathcal{F}_{\mathrm{inter}} + \mathcal{F}_{\mathrm{coll}}$ plus the constraint term $(2\pi\gamma/R_{\mathrm{drop}})\mu\Delta V$ (where μ is a dimensionless Lagrange multiplier):

$$\mathcal{F} = 2\pi\gamma \int_{\psi_0}^{\psi_1} d\psi \sin\psi \left[\frac{1}{2}\left(\frac{du}{d\psi}\right)^2 - u^2 + \mu R_{\mathrm{drop}} u - \frac{R_{\mathrm{drop}}^2}{\gamma}\Pi u \right] + \pi\gamma[u_0 - \Delta h]^2 - F\Delta h. \tag{B6}$$

The quantity $-\gamma\mu/R_{\mathrm{drop}}$ can be interpreted as a homogeneous pressure field enforcing the constant-volume constraint. We note that the terms linear in u present in Eqs. (B2) and (B3) have cancelled in the total free energy. Minimization with respect to Δh yields the same result as in Eq. (14). Subsequent minimization with respect to $u(\psi)$ leads to

$$\frac{1}{\sin\psi}\frac{d}{d\psi}\left(\sin\psi\frac{du}{d\psi}\right) + 2u = -\frac{R_{\mathrm{drop}}^2}{\gamma}\Pi + \mu R_{\mathrm{drop}} \tag{B7}$$

and [compare with Eq. (17)]

$$\left.\frac{du}{d\psi}\right|_{\psi_0} = \varepsilon_F R_{\mathrm{drop}}. \tag{B8}$$

The solution must satisfy the constant-volume constraint

$$\int_{\psi_0}^{\psi_1} d\psi \sin\psi u(\psi) = 0. \tag{B9}$$

Finally, the second boundary condition mentioned at the beginning expresses the physical requirement that the droplet is fixed in space. (Otherwise, the application of a localized force at the interface would shift the droplet as a whole without deforming it.) As an example, we assume that the droplet interface is pinned at ψ_1 (another example, force balance by suitable localized counterstresses, is studied in Ref. [35]):

$$u(\psi = \psi_1) = 0. \tag{B10}$$

The general solution of the inhomogeneous Legendre Eq. (B7) is

$$u(\psi) = AP(\psi) + BQ(\psi) + \frac{1}{2}\mu R_{\mathrm{drop}} + \frac{R_{\mathrm{drop}}^2}{\gamma}\int_{\psi}^{\psi_1} d\sigma \sin\sigma[P(\sigma)Q(\psi) - P(\psi)Q(\sigma)]\Pi(\sigma), \tag{B11}$$

where A and B are integration constants and

$$P(\psi) := \cos\psi,$$

$$Q(\psi) := 1 + \cos\psi \ln\tan\frac{\psi}{2}, \tag{B12}$$

are solutions of the homogeneous Legendre equation. For notational simplicity, evaluation of a function at $\psi_0(\psi_1)$ will be denoted by the subscript $_{0(1)}$.

From Eq. (B10) one obtains

$$\tfrac{1}{2}\mu R_{\mathrm{drop}} = -AP_1 - BQ_1. \tag{B13}$$

From the other boundary condition (B8) it follows that

$$\varepsilon_F R_{\mathrm{drop}} = AP'_0 + BQ'_0 + \frac{R_{\mathrm{drop}}^2}{\gamma}\int_{\psi_0}^{\psi_1} d\sigma \sin\sigma W(\sigma)\Pi(\sigma), \tag{B14}$$

where we have defined the auxiliary function

$$W(\sigma) := [P(\sigma)Q'_0 - P'_0 Q(\sigma)]. \tag{B15}$$

Finally, in order to impose the integral constraint (B9) we employ the following identities:

$$\begin{aligned}\int_{\psi_0}^{\psi_1} d\psi \sin\psi \int_{\psi}^{\psi_1} d\sigma \sin\sigma[P(\sigma)Q(\psi) - P(\psi)Q(\sigma)]\Pi(\sigma) &= \int_{\psi_0}^{\psi_1} d\sigma \sin\sigma\Pi(\sigma)\int_{\psi_0}^{\sigma} d\psi \sin\psi[P(\sigma)Q(\psi) - P(\psi)Q(\sigma)] \\ &= -\int_{\psi_0}^{\psi_1} d\sigma \sin\sigma\Pi(\sigma)\frac{1}{2}\left[1 - \frac{W(\sigma)}{W_0}\right].\end{aligned} \tag{B16}$$

The first equality follows from interchanging the order of integration. The last equality follows most easily by noticing (i) that the ψ integral in the second line is, as a function of σ, a solution of the differential Eq. (B7) with u replaced by this integral, μR_{drop} replaced by -1, $\Pi = 0$, and the analogs of the boundary conditions $u_0 = 0 = u'_0$, and (ii) that the function $(W(\sigma)/W_0 - 1)/2$ is the solution to the same differential equation with the same boundary conditions. With these identities Eq. (B9) turns into

$$0 = A\mathcal{P} + B\mathcal{Q} - \frac{R_{\mathrm{drop}}^2}{2\gamma}\int_{\psi_0}^{\psi_1} d\sigma \sin\sigma\Pi(\sigma)\left[1 - \frac{W(\sigma)}{W_0}\right], \tag{B17}$$

where we have introduced the numerical constants

$$\mathcal{P} := \int_{\psi_0}^{\psi_1} d\psi \sin\psi[P(\psi) - P_1]$$

$$\mathcal{Q} := \int_{\psi_0}^{\psi_1} d\psi \sin\psi[Q(\psi) - Q_1]. \tag{B18}$$

We note that the constants A and B are determined by the two linear Eqs. (B14) and (B17).

These results permit us to study the intermediate asymptotic regime $r_{0,\mathrm{ref}}, r \ll R_{\mathrm{drop}}$. In the expressions derived above, we have to take the limit $R_{\mathrm{drop}} \to \infty$ while keeping fixed ψ_1, $r = R_{\mathrm{drop}}\psi$ and $r_{0,\mathrm{ref}} = R_{\mathrm{drop}}\psi_0$ (so that $\psi_0, \psi \ll 1$). In this limit, the constants $\mathcal{P}$ and $\mathcal{Q}$ are finite, while $P(\psi) \simeq 1$ and $Q(\psi) \simeq \ln(r/R_{\mathrm{drop}}) - \ln 2 + 1$. The integrals over Π appearing in Eqs. (B11), (B14), and (B17) are simplified when the stress field $\Pi(\psi)$ decays sufficiently fast. So, e.g.,

$$\int_{\psi_0}^{\psi_1} d\sigma \sin\sigma W(\sigma)\Pi(\sigma)$$
$$= \frac{1}{R_{\text{drop}}}\int_{r_{0,\text{ref}}}^{\psi_1 R_{\text{drop}}} ds \sin\left(\frac{s}{R_{\text{drop}}}\right) W\left(\frac{s}{R_{\text{drop}}}\right)\Pi\left(\frac{s}{R_{\text{drop}}}\right)$$
$$\simeq \frac{1}{R_{\text{drop}}^2}\left(\frac{R_{\text{drop}}}{r_{0,\text{ref}}}\right)\int_{r_{0,\text{ref}}}^{+\infty} ds s \Pi\left(\frac{s}{R_{\text{drop}}}\right), \tag{B19}$$

since the main contribution of the integrand stems from the region $s/R_{\text{drop}} \ll 1$, in which $W(s/R_{\text{drop}}) \simeq R_{\text{drop}}/r_{0,\text{ref}}$. In this manner, we obtain from Eq. (B14):

$$B \simeq r_0(\varepsilon_F - \varepsilon_\Pi), \tag{B20}$$

and Eq. (B17) yields

$$A \simeq -\frac{\mathcal{Q}}{\mathcal{P}} r_0(\varepsilon_F - \varepsilon_\Pi). \tag{B21}$$

One finds indeed that the Lagrange multiplier μ determined by Eq. (B13) is linear in $\varepsilon_F - \varepsilon_\Pi$. Finally, the general solution (B11) simplifies to

$$u \simeq A(1-P_1) + B\left(\ln\frac{r}{R_{\text{drop}}} - \ln 2 + 1 - Q_1\right)$$
$$-\frac{1}{\gamma}\int_r^{+\infty} ds s \Pi\left(\frac{s}{R_{\text{drop}}}\right)\ln\frac{s}{r}, \tag{B22}$$

which renders Eq. (24) with the constant

$$\tilde{C} = 2\exp\left[(1-P_1)\frac{\mathcal{Q}}{\mathcal{P}} + Q_1 - 1\right]. \tag{B23}$$

This constant is finite and non-vanishing provided ψ_1 is not close to π. The case $\psi_1 = \pi$ is pathological because $u'(\pi) \equiv 0$ for a smooth profile, so that the boundary condition (B10) would overdetermine the problem.

[1] P. Pieranski, Phys. Rev. Lett. **45**, 569 (1980).
[2] J. D. Joannopoulos, Nature (London) **414**, 257 (2001).
[3] A. D. Dinsmore, M. F. Hsu, M. G. Nikolaides, M. Márquez, A. R. Bausch, and D. A. Weitz, Science **298**, 1006 (2002).
[4] A. Hurd, J. Phys. A **18**, L1055 (1985).
[5] R. Aveyard, B. P. Binks, J. H. Clint, P. D. I. Fletcher, T. S. Horozov, B. Neumann, V. N. Paunov, J. Annesley, S. W. Botchway, D. Nees, A. W. Parker, A. D. Ward, and A. N. Burgess, Phys. Rev. Lett. **88**, 246102 (2002).
[6] F. Ghezzi and J. C. Earnshaw, J. Phys.: Condens. Matter **9**, L517 (1997).
[7] F. Ghezzi, J. C. Earnshaw, M. Finnis, and M. McCluney, J. Colloid Interface Sci. **238**, 433 (2001).
[8] J. Ruiz-García and B. I. Ivlev, Mol. Phys. **95**, 371 (1998).
[9] J. Ruiz-García, R. Gámez-Corrales, and B. I. Ivlev, Phys. Rev. E **58**, 660 (1998).
[10] D. Stamou, C. Duschl, and D. Johannsmann, Phys. Rev. E **62**, 5263 (2000).
[11] M. Quesada-Pérez, A. Moncho-Jordá, F. Martínez-López, and R. Hidalgo-Alvarez, J. Chem. Phys. **115**, 10897 (2001).
[12] M. G. Nikolaides, A. R. Bausch, M. F. Hsu, A. D. Dinsmore, M. P. Brenner, C. Gay, and D. A. Weitz, Nature (London) **420**, 299 (2002).
[13] M. Megens and J. Aizenberg, Nature (London) **420**, 1014 (2003).
[14] M. G. Nikolaides, A. R. Bausch, M. F. Hsu, A. D. Dinsmore, M. P. Brenner, C. Gay, and D. A. Weitz, Nature (London) **424**, 1014 (2003).
[15] L. Foret and A. Würger, Phys. Rev. Lett. **92**, 058302 (2004).
[16] K. D. Danov, P. A. Kralchevsky, and M. P. Boneva, Langmuir **20**, 6139 (2004).
[17] P. A. Kralchevsky and K. Nagayama, Adv. Colloid Interface Sci. **85**, 145 (2000).
[18] A. I. Shestakov, J. L. Milovich, and A. Noy, J. Colloid Interface Sci. **247**, 62 (2002).
[19] R. Courant and D. Hilbert, *Methods of Mathematical Physics* (Wiley, New York, 1989), Vol. 1.
[20] *Handbook of Mathematical Functions*, edited by M. Abramowitz and I. A. Stegun (Dover, New York, 1974).
[21] G. I. Barenblatt, *Scaling, Self-Similarity, and Intermediate Asymptotics* (Cambridge University Press, Cambridge, 1996).
[22] N. Goldenfeld, *Lectures on Phase Transitions and the Renormalization Group* (Addison-Wesley, Reading, MA, 1992).
[23] P. A. Kralchevsky, V. N. Paunov, I. B. Ivanov, and K. Nagayama, J. Colloid Interface Sci. **151**, 79 (1991).
[24] M. M. Nicolson, Proc. Cambridge Philos. Soc. **45**, 288 (1949).
[25] V. N. Paunov, P. A. Kralchevsky, N. D. Denkov, and K. Nagayama, J. Colloid Interface Sci. **157**, 100 (1993).
[26] D. Y. C. Chan, J. D. Henry, Jr., and L. R. White, J. Colloid Interface Sci. **79**, 410 (1981).
[27] D. J. Robinson and J. C. Earnshaw, Langmuir **9**, 1436 (1993).
[28] D. Gouldin and J.-P. Hansen, Mol. Phys. **95**, 649 (1998).
[29] R. Aveyard, J. H. Clint, D. Nees, and V. N. Paunov, Langmuir **16**, 1969 (2000).
[30] M. K. Gilson, M. E. Davis, B. A. Luty, and J. A. McCammon, J. Phys. Chem. **97**, 3591 (1993).
[31] M. G. Nikolaides and A. Bausch (private communication).
[32] J. C. Fernández-Toledano, A. Moncho-Jordá, F. Martínez-López, and R. Hidalgo-Alvarez, Langmuir **20**, 6977 (2004).
[33] R. Golestanian, M. Goulian, and M. Kardar, Phys. Rev. E **54**, 6725 (1996).
[34] I. I. Smalyukh, S. Chernyshuk, B. I. Lev, A. B. Nych, U. Ognysta, V. G. Nazarenko, and O. D. Lavrentovich, Phys. Rev. Lett. **93**, 117801 (2004).
[35] D. C. Morse and T. A. Witten, Europhys. Lett. **22**, 549 (1993).